

Track Coalescence and Repulsion: MHT, JPDA, and BP

Thomas Kropfreiter*, Florian Meyer*, Stefano Coraluppi[†], Craig Carthel[†], Rico Mendrzik[‡], and Peter Willett[§]

*Scripps Institution of Oceanography and Department of Electrical and Computer Engineering
University of California San Diego, La Jolla, CA, USA ({flmeyer, tkropfreiter}@ucsd.edu)

[†]Systems & Technology Research, Woburn, MA, USA ({stefano.coraluppi, craig.carthel}@stresearch.com)

[‡]Ibeo Automotive Systems GmbH, Hamburg, Germany (rico.mendrzik@ibeo-as.com)

[§]Department of ECE, University of Connecticut, Storrs, CT, USA (peter.willett@uconn.edu)

Abstract—Joint probabilistic data association (JPDA) and multiple hypothesis tracking (MHT) introduced in the 70s, are still widely used methods for multitarget tracking (MTT). Extensive studies over the last few decades have revealed undesirable behavior of JPDA and MHT type methods in tracking scenarios with targets in close proximity. In particular, JPDA suffers from the track coalescence effect, i.e., estimated tracks of targets in close proximity tend to merge and can become indistinguishable. Interestingly, in MHT, an opposite effect to track coalescence called track repulsion can be observed. In this paper, we review the estimation strategies of the MHT, JPDA, and the recently introduced belief propagation (BP) framework for MTT and we investigate if BP also suffers from these two detrimental effects. Our numerical results indicate that BP-based MTT can mostly avoid both track repulsion and coalescence.

Index Terms—Multitarget tracking, joint probabilistic data association, multiple hypothesis tracking, belief propagation

I. INTRODUCTION

Multitarget tracking (MTT) [1]–[5] is a key signal processing task that enables situational awareness in a variety of applications. Historically, the most important MTT scenarios are aerospace surveillance [6]–[8] and applied ocean sciences [9]–[11]. However, in the context of autonomous navigation, robotic applications are recently drawing increased attention [12], [13]. MTT methods are typically derived in the Bayesian estimation framework and they rely on different modeling paradigms, which can be broadly classified as vector-type [14]–[24] and set-type [25]–[29].

Vector-type MTT methods describe both multitarget states and measurements by random vectors. The well-known joint probabilistic data association (JPDA) filter [7] introduced in the 70s established the probabilistic data association (DA) paradigm for MTT. The JPDA aims to calculate the minimum mean square error (MMSE) state estimates for a known number of targets. Data association hypotheses are employed in a soft manner by performing weighted sums over all possible associations at each time step. Performing these weighted sums is equivalent to calculate the marginal posterior probability density functions needed for state estimation by “marginalizing out” the unknown data association vector. In contrast, the very popular multiple hypothesis tracking (MHT) methods [6] seek to calculate the maximum a posteriori (MAP) estimate of an

entire sequence of data association vectors. In particular, MHT methods perform hard data association based on the single most likely measurement-target combination over multiple consecutive instances of time [6]. After an approximate MAP estimate of the data association vectors has been fixed, MAP or MMSE estimates of the target states can be calculated individually by means of sequential Bayesian estimation, e.g., extended Kalman filtering.

Extensive studies over the last few decades have revealed undesirable behavior of JPDA and MHT type methods in tracking scenarios with targets in close proximity. In particular, JPDA type methods suffer from the track coalescence effect [30], i.e., estimated tracks of closely spaced targets that move in parallel will tend to come together, merge, and can become indistinguishable. Interestingly, in MHT, an opposite effect to track coalescence called track repulsion [31] can be observed. In particular, estimated tracks of close targets that move in parallel repel each other in the sense that their separation is larger compared to the distance between the actual targets. Methodological adaptations tailored to alleviate these detrimental effects have been introduced in [32]–[35]. Track coalescence can be avoided by using a special hypothesis pruning strategy [32], [33] and track repulsion by selecting a global hypothesis that is not the single MAP solution, but an element of a MAP equivalence class [34]. While these adaptations can reduce the effects of track coalescence and repulsion, they are unsuitable for large-scale tracking scenarios with an unknown and time-varying number of targets.

Set-type methods describe both multitarget states and measurements by random finite sets. Some approaches in this class including probability hypothesis density (PHD) methods [25]–[27], [29] avoid data association at the cost of a reduced target detection and tracking performance as well as a suboptimal postprocessing step for track formation. Some other RFS methods rely on association strategies similar to the ones performed by the JPDA filter and thus also suffer from track coalescence [28], [36].

Recently developed graph signal processing methods for MTT [5], [13], [37], [38] fit in the vector-type family. Here, filtering and data association for randomly appearing and disappearing targets are described by a joint factor graph.

This factor graph provides the blueprint for sum-product message passing algorithms also known as belief propagation (BP). By following the MMSE estimation approach of the JPDA, BP performs efficient marginalization operations and can provide scalable solutions to two pertinent problems: the data association problem that arises due to measurement-origin uncertainty and the presence of clutter as well as the nonlinear filtering problem with appearing and disappearing target states.

In this paper, we review the track coalescence and repulsion effects of the JPDA and MHT methods and investigate them in the context of BP-based MTT. The contributions of this paper are as follows.

- We review the estimation strategies of the MHT, JPDA, and BP approaches to MTT.
- We discuss the track coalescence and track repulsion effects of MHT, JPDA, and BP.
- We demonstrate significantly reduced track coalescence and repulsion of BP in three different case studies.

Notation: Random variables are displayed in sans serif, upright fonts; their realizations in serif, italic fonts. Vectors and matrices are denoted by bold lowercase and uppercase letters, respectively. For example, a random variable and its realization are denoted by \mathbf{x} and x and a random vector and its realization by \mathbf{x} and \mathbf{x} . Furthermore, \mathbf{x}^T denotes the transpose of vector \mathbf{x} ; \propto indicates equality up to a normalization factor; $f(\mathbf{x})$ denotes the probability density function (pdf) of random vector \mathbf{x} . Finally, $1(a)$ denotes the unit sample function (i.e., $1(a) = 1$ if $a = 0$ and 0 otherwise).

II. GENERAL SYSTEM MODEL

In this section, we introduce a general MTT system model.

A. Potential Target States and State-Transition PDF

In most practical applications, the number of targets is time-varying and unknown. Here, we introduce potential target (PT) states [5], [38]. At discrete time $k \geq 0$, the number of PTs j_k is the maximum possible number of targets that have generated a measurement. The state of PT $j \in \{1, \dots, j_k\}$ consists of a binary existence variable $r_k^{(j)} \in \{0, 1\}$ and a kinematic state $\mathbf{x}_k^{(j)} \in \mathbb{R}^n$. The existence variable $r_k^{(j)}$ models the existence/nonexistence of PT j in the sense that PT j exists at time k if and only if $r_k^{(j)} = 1$. The state $\mathbf{x}_k^{(j)}$ of PT j consists of the PT's position and possibly further motion-related parameters.

The kinematic state $\mathbf{x}_k^{(j)}$ of PTs with $r_k^{(j)} = 0$ is not defined and can be represented by an arbitrary “dummy” pdf $f_D(\mathbf{x}_k^{(j)})$ with $\int f_D(\mathbf{x}_k^{(j)}) d\mathbf{x}_k^{(j)} = 1$. All pdfs of PT states, $f(\mathbf{x}_k^{(j)}, r_k^{(j)})$, have the property that $f(\mathbf{x}_k^{(j)}, 0) = f_k^{(j)} f_D(\mathbf{x}_k^{(j)})$, where $f_k^{(j)} \in [0, 1]$ is the probability of nonexistence. For each PT state $(\mathbf{x}_{k-1}^{(j)}, r_{k-1}^{(j)})$, $j \in \{1, \dots, j_{k-1}\}$ at time $k-1$, there is one “legacy” PT state $(\mathbf{x}_k^{(j)}, r_k^{(j)})$ at time k . The motion and disappearance of each PT is modeled by the single-target state-transition pdf $f(\mathbf{x}_k^{(j)}, r_k^{(j)} | \mathbf{x}_{k-1}^{(j)}, r_{k-1}^{(j)})$ that involves the kinematic state-transition pdf $f(\mathbf{x}_k^{(j)} | \mathbf{x}_{k-1}^{(j)})$ and

the probability of target survival p_s (e.g., see [5, Section VIII-C]). It is assumed that each target evolves independently. At time $k = 0$, the target states are assumed statistically independent across PTs j . However, often no prior information for PT states is available, i.e., $j_0 = 0$.

B. New PTs, Data Association, and Measurement Likelihood Function

At each time (or “scan”) $k \geq 1$, a sensor produces measurements $\mathbf{z}_k^{(m)}$, $m \in \{1, \dots, m_k\}$. (Note that up to time k , the number of measurements m_k is random.) Each measurement can have one of three possible sources: (i) a new PT representing a target that generates a measurement for the first time; (ii) a legacy PT representing a target that has generated at least one measurement before; and (iii) clutter. At time k , m_k new PT states are introduced, i.e., $(\bar{\mathbf{x}}_k^{(m)}, \bar{r}_k^{(m)})$, $m \in \{1, \dots, m_k\}$. Here, $\bar{r}_k^{(m)} = 1$ means that measurement $\mathbf{z}_k^{(m)}$ has source (i) and $\bar{r}_k^{(m)} = 0$ means that measurement $\mathbf{z}_k^{(m)}$ has either source (ii) or (iii). The birth of new targets is modeled by a Poisson point process with mean μ_b and pdf $f_b(\bar{\mathbf{x}}_k)$. The joint vectors of all existence variables and kinematic states at time k are denoted as $\mathbf{x}_k = [\mathbf{x}_k^{(1)} \dots \mathbf{x}_k^{(j_{k-1})} \bar{\mathbf{x}}_k^{(1)} \dots \bar{\mathbf{x}}_k^{(m_k)}]^T$ and $\mathbf{r}_k = [r_k^{(1)} \dots r_k^{(j_{k-1})} \bar{r}_k^{(1)} \dots \bar{r}_k^{(m_k)}]^T$, respectively.

The target represented by a PT j is detected (in the sense that it generates a measurement $\mathbf{z}_k^{(m)}$) with probability p_d . The statistical relationship of a measurement $\mathbf{z}_k^{(m)}$ and the kinematic state $\mathbf{x}_k^{(j)}$ of the corresponding detected PT, is described by the conditional pdf $f(\mathbf{z}_k^{(m)} | \mathbf{x}_k^{(j)})$. This conditional pdf can be derived from the measurement model of the sensor. Clutter measurements are modeled by a Poisson point process with mean μ_c and pdf $f_c(\mathbf{z}_k^{(m)})$. At time k , the joint measurement vector is fixed and denoted as $\mathbf{z}_k \triangleq [\mathbf{z}_k^{(1)} \dots \mathbf{z}_k^{(m_k)}]^T$. Thus, the total number of (legacy and new) PTs is $j_k = j_{k-1} + m_k$.

In MTT, the source of measurements is uncertain. In particular, it is unknown which measurement is generated by which PT, and a measurement may also be clutter, i.e., not generated by any PT. The considered MTT problem follows the conventional DA assumption, i.e., a target can originate at most one measurement and a measurement can be originated from at most one target [1], [3], [5]. The association between m_k measurements and j_{k-1} legacy PTs at time k is typically modeled by a “target-oriented” DA vector $\mathbf{a}_k = [\mathbf{a}_k^{(1)} \dots \mathbf{a}_k^{(j_{k-1})}]^T$. The target-oriented association variable $\mathbf{a}_k^{(j)}$ is $m \in \{1, \dots, m_k\}$ if PT j originated measurement m and zero if PT j did not originate any measurement [1], [5]. A DA vector \mathbf{a}_k is valid if it does not violate the conventional DA association assumption.

We also introduce the “measurement-oriented” DA vector $\mathbf{b}_k = [\mathbf{b}_k^{(1)} \dots \mathbf{b}_k^{(m_k)}]^T$. The measurement-oriented association variable $\mathbf{b}_k^{(m)}$ is $j \in \{1, \dots, j_{k-1}\}$ if measurement m is generated by legacy PT j and zero if it is generated by clutter or by a newly detected PT. The DA representation by means of both target-oriented and measurement-oriented DA vectors is redundant in the sense that for any valid \mathbf{a}_k , there is exactly one valid \mathbf{b}_k and for any valid \mathbf{b}_k , there is

exactly one valid \mathbf{a}_k . However, this representation based on both \mathbf{a}_k and \mathbf{b}_k makes it possible to develop scalable MTT methods that exploit the structure of the DA problem to reduce computational complexity.

C. Joint Posterior PDF and Factor Graph

Following common assumptions [1], [3], [5], [6], [28], [37]–[39], the joint posterior pdf of $\mathbf{x}_{0:k}$, $\mathbf{r}_{0:k}$, $\mathbf{a}_{1:k}$, and $\mathbf{b}_{1:k}$ conditioned on fixed measurements $\mathbf{z}_{1:k}$ can be obtained as

$$\begin{aligned} & f(\mathbf{x}_{0:k}, \mathbf{r}_{0:k}, \mathbf{a}_{1:k}, \mathbf{b}_{1:k} | \mathbf{z}_{1:k}) \\ & \propto \left(\prod_{j'=1}^{j_0} f(\mathbf{x}_0^{(j')}, \mathbf{r}_0^{(j')}) \right) \prod_{k'=1}^k \\ & \quad \times \left(\prod_{j'=1}^{j_{k'}-1} f(\mathbf{x}_{k'}^{(j')}, \mathbf{r}_{k'}^{(j')} | \mathbf{x}_{k'-1}^{(j')}, \mathbf{r}_{k'-1}^{(j')}) \right) \\ & \quad \times \left(\prod_{j=1}^{j_{k'}-1} q(\mathbf{x}_{k'}^{(j)}, \mathbf{r}_{k'}^{(j)}, \mathbf{a}_{k'}^{(j)}; \mathbf{z}_{k'}) \prod_{m'=1}^{m_{k'}} \Psi_{j,m'}(\mathbf{a}_{k'}^{(j)}, \mathbf{b}_{k'}^{(m')}) \right) \\ & \quad \times \prod_{m=1}^{m_{k'}} v(\mathbf{x}_{k'}^{(m)}, \mathbf{r}_{k'}^{(m)}, \mathbf{b}_{k'}^{(m)}; \mathbf{z}_{k'}^{(m)}). \end{aligned} \quad (1)$$

Here, the new PT factor $v(\mathbf{x}_k^{(m)}, \mathbf{r}_k^{(m)}, \mathbf{b}_k^{(m)}; \mathbf{z}_k^{(m)})$ is given by

$$\begin{aligned} & v(\mathbf{x}_k^{(m)}, \mathbf{r}_k^{(m)}, \mathbf{b}_k^{(m)}; \mathbf{z}_k^{(m)}) \\ & \triangleq \begin{cases} 0, & \mathbf{b}_k^{(m)} \in \{1, \dots, j_{k-1}\} \\ \frac{p_d \mu_b f_b(\mathbf{x}_k^{(m)})}{\mu_c f_c(\mathbf{z}_k^{(m)})} f(\mathbf{z}_k^{(m)} | \mathbf{x}_k^{(m)}), & \mathbf{b}_k^{(m)} = 0 \end{cases} \end{aligned}$$

and $v(\mathbf{x}_k^{(m)}, 0, \mathbf{b}_k^{(m)}; \mathbf{z}_k^{(m)}) \triangleq f_D(\mathbf{x}_k^{(m)})$. In addition, the legacy PT factor $q(\mathbf{x}_k^{(j)}, \mathbf{r}_k^{(j)}, \mathbf{a}_k^{(j)}; \mathbf{z}_k)$ reads

$$\begin{aligned} & q(\mathbf{x}_k^{(j)}, \mathbf{r}_k^{(j)}, \mathbf{a}_k^{(j)}; \mathbf{z}_k) \\ & \triangleq \begin{cases} \frac{p_d}{\mu_c f_c(\mathbf{z}_k^{(m)})} f(\mathbf{z}_k^{(m)} | \mathbf{x}_k^{(j)}), & \mathbf{a}_k^{(j)} = m \in \{1, \dots, m_k\} \\ 1 - p_d, & \mathbf{a}_k^{(j)} = 0 \end{cases} \end{aligned}$$

and $q(\mathbf{x}_k^{(j)}, 0, \mathbf{a}_k^{(j)}; \mathbf{z}_k) \triangleq 1(a_k^{(j)})$.

Finally, consistency of a pair of target-oriented and measurement-oriented variables $(\mathbf{a}_k^{(j)}, \mathbf{b}_k^{(m)})$ is checked by the binary indicator function $\Psi_{j,m}(\mathbf{a}_k^{(j)}, \mathbf{b}_k^{(m)})$. In particular, $\Psi_{j,m}(\mathbf{a}_k^{(j)}, \mathbf{b}_k^{(m)})$ is zero if $\mathbf{a}_k^{(j)} = m, \mathbf{b}_k^{(m)} \neq j$ or $\mathbf{b}_k^{(m)} = j, \mathbf{a}_k^{(j)} \neq m$ and one otherwise (see [5], [37] for details). A detailed derivation of the joint posterior in (1) has been introduced in [5, Section VIII-G].

After marginalizing out $\mathbf{b}_{1:k}$ in (1), the resulting posterior distribution

$$f(\mathbf{x}_{0:k}, \mathbf{r}_{0:k}, \mathbf{a}_{1:k} | \mathbf{z}_{1:k}) = \sum_{\mathbf{b}_{1:k}} f(\mathbf{x}_{0:k}, \mathbf{r}_{0:k}, \mathbf{a}_{1:k}, \mathbf{b}_{1:k} | \mathbf{z}_{1:k}) \quad (2)$$

represents a system model that is identical to the one used by the MHT¹ and a more general version of the one used by JPDA methods. Note that this marginalization is trivial since for $\mathbf{a}_{1:k}$ there is exactly one $\mathbf{b}_{1:k}$ for which (1) is nonzero.

III. MULTITARGET TRACKING STRATEGIES

In this section, we will review the different estimation strategies of the MHT, the JPDA, and the BP methods and discuss how they can cause track repulsion and track coalescence.

A. MHT for Sequence MAP Estimation

MHT tracking aims to compute the sequence MAP estimate of $\mathbf{x}_{0:k}, \mathbf{r}_{0:k}, \mathbf{a}_{1:k}$ given $\mathbf{z}_{1:k}$. In particular, first the sequence MAP of $\mathbf{r}_{0:k}, \mathbf{a}_{1:k}$ given $\mathbf{z}_{1:k}$ is computed as

$$(\hat{\mathbf{r}}_{0:k}^{\text{MAP}}, \hat{\mathbf{a}}_{1:k}^{\text{MAP}}) = \arg \max_{\mathbf{r}_{0:k}, \mathbf{a}_{1:k}} \int f(\mathbf{x}_{0:k}, \mathbf{r}_{0:k}, \mathbf{a}_{1:k} | \mathbf{z}_{1:k}) d\mathbf{x}_{0:k} \quad (3)$$

This is equivalent to searching for the most likely target-measurement association or global hypothesis [6]. The MHT exploits the fact that the marginalization operation $\int d\mathbf{x}_{0:k}$ can be performed sequentially and, assuming a linear-Gaussian state-transition and measurement model, also in closed form. The optimal MAP solution however is a “multi-scan solution” in the sense that the optimal estimate $(\hat{\mathbf{r}}_{0:k}^{\text{MAP}}, \hat{\mathbf{a}}_{1:k}^{\text{MAP}})$ at time k can potentially be completely different than the optimal estimate $(\hat{\mathbf{r}}_{0:k-1}^{\text{MAP}}, \hat{\mathbf{a}}_{1:k-1}^{\text{MAP}})$ at time $k-1$. Thus, for optimal MAP estimation it is necessary to keep track of an exponentially growing number of global hypotheses $(\mathbf{r}_{0:k}, \mathbf{a}_{1:k})$.

Given the most likely target-measurement association $(\hat{\mathbf{r}}_{0:k}^{\text{MAP}}, \hat{\mathbf{a}}_{1:k}^{\text{MAP}})$, the MHT then computes a MAP estimate of $\mathbf{x}_{0:k}$ as

$$\begin{aligned} \hat{\mathbf{x}}_{0:k}^{\text{MAP}} &= \arg \max_{\mathbf{x}_{0:k}} f(\mathbf{x}_{0:k} | \hat{\mathbf{r}}_{0:k}^{\text{MAP}}, \hat{\mathbf{a}}_{1:k}^{\text{MAP}}, \mathbf{z}_{1:k}) \\ &= \arg \max_{\mathbf{x}_{0:k}} f(\mathbf{x}_{0:k}, \hat{\mathbf{r}}_{0:k}^{\text{MAP}}, \hat{\mathbf{a}}_{1:k}^{\text{MAP}} | \mathbf{z}_{1:k}) \end{aligned} \quad (4)$$

Note that for $(\hat{\mathbf{r}}_{0:k}^{\text{MAP}}, \hat{\mathbf{a}}_{1:k}^{\text{MAP}})$ fixed, the joint posterior (2) can be split into independent posterior distributions (one for each detected target according to $\hat{\mathbf{r}}_{0:k}^{\text{MAP}}$, cf. (1)). The joint target state estimate $\hat{\mathbf{x}}_{0:k}^{\text{MAP}}$ is then obtained by performing Bayesian smoothing for each detected target in parallel and independent of all other targets, e.g., by means of the Kalman smoother.

In a practical implementation, MHT computes the MAP estimates of the target-measurement association in (3) and of the target state in (4) only over a sliding window of N consecutive times steps in order to reduce the computational burden. A hard decision is then made only on the association at the oldest time step. MHT can be formulated in form of hypothesis-oriented MHT [6] and track-oriented MHT [21]–[23]. The computational complexity of the original hypothesis-oriented MHT formulation is still problematic due to the high number of hypotheses. However, it can be reduced by discarding unlikely hypotheses using, e.g., an efficient m -best assignment algorithm [19], [20].

¹In the MHT literature, the two vectors $\mathbf{r}_{0:k}$ and $\mathbf{a}_{1:k}$ are typically represented by an equivalent single vector $\mathbf{q}_{0:k}$ referred to as global hypothesis.

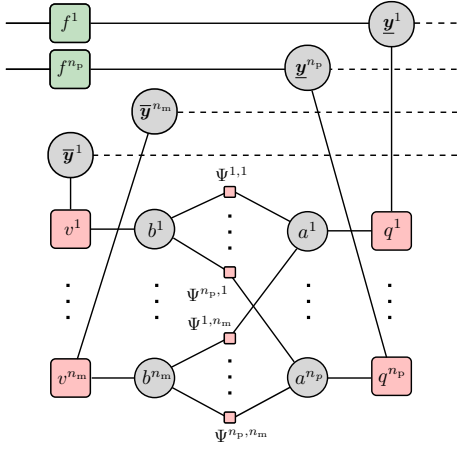


Fig. 1: Factor graph for an unknown, time-varying number of objects, corresponding to the joint posterior pdf $f(\mathbf{x}_{0:k}, \mathbf{r}_{0:k}, \mathbf{a}_{1:k}, \mathbf{b}_{1:k} | \mathbf{z}_{1:k})$ in (1). The factor graph depicts one time step k . The time index k is omitted, and the following short notations are used: $n_m \triangleq m_k$, $n_p \triangleq j_{k-1}$, $\mathbf{y}^j \triangleq [\mathbf{x}_k^{(j)}, \mathbf{r}_k^{(j)}]^T$, $\mathbf{y}^m \triangleq [\mathbf{x}_k^{(m)}, \mathbf{r}_k^{(m)}]^T$, $\mathbf{a}^j \triangleq \mathbf{a}_k^{(j)}$, $\mathbf{b}^m \triangleq \mathbf{b}_k^{(m)}$, $f^j \triangleq f(\mathbf{x}_k^{(j)}, \mathbf{r}_k^{(j)} | \mathbf{x}_{k-1}^{(j)}, \mathbf{r}_{k-1}^{(j)})$, $q^j \triangleq q(\mathbf{x}_k^{(j)}, \mathbf{r}_k^{(j)}, \mathbf{a}_k^{(j)}; \mathbf{z}_k)$, $v^m \triangleq v(\mathbf{x}_k^{(m)}, \mathbf{r}_k^{(m)}, \mathbf{b}_k^{(m)}; \mathbf{z}_k)$, $\Psi_{j,m}^{j,m} \triangleq \Psi_{j,m}(\mathbf{a}_k^{(j)}, \mathbf{b}_k^{(m)})$.

The more efficient track-oriented MHT methods [21]–[23] represent association hypotheses via a series of tree structures. Here, each tree represents the possible association histories of a single target. The most likely hypothesis is then found by choosing a leaf node for each single-target tree in such a way that no measurement is used by more than one target. Fast hypothesis-search is enabled by means of combinatorial optimization methods [24], [40]–[42]. Track-oriented MHT offers a more compact representation of the data association problem than hypothesis-oriented MHT. The two formulations are equivalent under the assumption that target births and clutter follow a Poisson point process [43].

A limitation of MHT tracking is known as track repulsion, which can arise when targets come in close proximity. It is a direct consequence of performing hard data association by considering only a single global hypothesis ($\hat{\mathbf{r}}_{0:k}^{\text{MAP}}, \hat{\mathbf{a}}_{1:k}^{\text{MAP}}$) for target state estimation according to (4). Estimated tracks are displaced at a greater distance than the targets themselves and thus result in an increased estimation error. This displacement can also lead to track swaps (or identity switches) [44], [45]. In a crossing target scenario the corresponding estimated tracks have the tendency to “bounce” more often than they cross. A method for mitigating the detrimental effects of track repulsion has been presented in [34].

B. JPDA for Marginal MMSE-Estimation

JPDA methods are based on the MMSE estimation criterion. (An exception is the set JPDA (SJPDA) filter [35], which aims to minimize the mean optimal sub-pattern assignment metric.) In particular, the JPDA aims to calculate MMSE estimates for each individual target state $\mathbf{x}_k^{(j)}$, i.e.,

$$\hat{\mathbf{x}}_k^{(j)\text{MMSE}} = \int \mathbf{x}_k^{(j)} f(\mathbf{x}_k^{(j)} | \mathbf{z}_{1:k}) d\mathbf{x}_k, \quad j = 1, \dots, l_k. \quad (5)$$

Contrary to MHT, in conventional JPDA it is assumed that the true sequence of existence variables $\hat{\mathbf{r}}_{0:k}$ (and thus the number of targets l_k at time k) is known, i.e.,

$$f(\mathbf{x}_{0:k}, \mathbf{a}_{1:k} | \mathbf{z}_{1:k}) \propto f(\mathbf{x}_{0:k}, \hat{\mathbf{r}}_{0:k}, \mathbf{a}_{1:k} | \mathbf{z}_{1:k}). \quad (6)$$

The marginals needed for optimum state estimation in (5) are then calculated from (6) according to

$$f(\mathbf{x}_k^{(j)} | \mathbf{z}_{1:k}) = \int \sum_{\mathbf{a}_{1:k}} f(\mathbf{x}_{0:k}, \mathbf{a}_{1:k} | \mathbf{z}_{1:k}) d\mathbf{x}_{0:k}^{(j)}, \quad (7)$$

where $\mathbf{x}_{0:k}^{(j)}$ denotes the vector that consists of all entries in $\mathbf{x}_{0:k}$ except $\mathbf{x}_k^{(j)}$. In practical implementations a track initialization and termination heuristic provides an approximate sequence of existence variables $\hat{\mathbf{r}}_{0:k}$. Under the assumption of linear and Gaussian measurement and motion models as used in the original formulation of the JPDA, approximate closed-form expressions for the marginalization (7) can be found. However, the summation over all joint associations hypotheses performed in (7) remains computationally infeasible in tracking scenarios with more than 7 targets. Further complexity reduction can be obtained by applying heuristic approximations [16], [46], by using efficient hypothesis management [17], or by limiting the number of target-measurement associations [18].

A deficiency of JPDA tracking is known as track coalescence, which can arise when targets come close to each other. In such situations, JPDA is unable to maintain awareness of target positions and the estimated tracks tend to merge, and can become indistinguishable. Track coalescence is a direct consequence of calculating marginal distributions $f(\mathbf{x}_k^{(j)} | \mathbf{z}_{1:k})$ for the individual target states according to (7). In particular, performing soft data association by means of the sum over all possible associations $\sum_{\mathbf{a}_k}$ for each time step k , has the effect that targets with identical prior distribution will also have identical posterior distribution. Consequently, as targets are in close proximity and their prior distributions become similar, their posterior distributions tend to merge. Mitigation methods include the pruning of association hypotheses [32], [33], approximate calculation of marginal pdfs via information-theoretic based optimization techniques [35], [47] or mean-field approximations [48].

C. BP for Marginal Detection and MMSE-Estimation

In BP-based multitarget tracking [5], [13], [38], [49], we aim to compute the marginal posterior pdfs $f(\mathbf{x}_k^{(j)}, \mathbf{r}_k^{(j)} | \mathbf{z}_{1:k})$ for each PT $j \in \{1, \dots, j_k\}$. From these marginal posterior pdfs, detection and MMSE estimation can be performed individually for each PT $j \in \{1, \dots, j_k\}$.

In particular, for each PT, marginal posterior probability mass functions $p(r_k^{(j)} | \mathbf{z}_{1:k})$ of the existence indicators $r_k^{(j)}$ are obtained from marginal posterior pdfs $f(\mathbf{x}_k^{(j)}, \mathbf{r}_k^{(j)} | \mathbf{z}_{1:k})$ as

$$p(r_k^{(j)} | \mathbf{z}_{1:k}) = \int f(\mathbf{x}_k^{(j)}, r_k^{(j)} | \mathbf{z}_{1:k}) d\mathbf{x}_k^{(j)}. \quad (8)$$

Targets are then declared to exist if $p(r_k^{(j)}=1|z_{1:k})$ is greater than a predefined threshold P_{th} . For all targets declared to exist, state estimation is performed by the MMSE estimator according to

$$\hat{\mathbf{x}}_k^{(j)\text{MMSE}} \triangleq \int \mathbf{x}_k \frac{f(\mathbf{x}_k, r_k^{(j)}=1|z_{1:k})}{p(r_k^{(j)}=1|z_{1:k})} d\mathbf{x}_k. \quad (9)$$

Let us first investigate the calculation of the joint marginal pdfs $f(\mathbf{x}_k, r_k | z_{1:k})$ that involves the joint state and existence variable of all targets at time k . A naive marginalization of (1) can be performed as

$$\begin{aligned} & f(\mathbf{x}_k, r_k | z_{1:k}) \\ &= \int \sum_{\mathbf{r}_{0:k-1}} \sum_{\mathbf{a}_{1:k}} \sum_{\mathbf{b}_{1:k}} f(\mathbf{x}_{0:k}, \mathbf{r}_{0:k}, \mathbf{a}_{1:k}, \mathbf{b}_{1:k} | z_{1:k}) d\mathbf{x}_{0:k-1}. \end{aligned} \quad (10)$$

By using (1) in (10) and marginalizing out the vectors $\mathbf{x}_{1:k-2}$, $\mathbf{r}_{1:k-2}$, $\mathbf{a}_{1:k-1}$, and $\mathbf{b}_{1:k-1}$, we obtain

$$\begin{aligned} & f(\mathbf{x}_k, r_k | z_{1:k}) \\ &= \int \sum_{\mathbf{r}_{k-1}} \sum_{\mathbf{a}_k} \sum_{\mathbf{b}_k} f(\mathbf{x}_{k-1}, \mathbf{r}_{k-1} | z_{1:k-1}) \\ & \quad \times g(\mathbf{x}_k, \mathbf{r}_k, \mathbf{x}_{k-1}, \mathbf{r}_{k-1}, \mathbf{a}_k, \mathbf{b}_k) d\mathbf{x}_{k-1} \end{aligned} \quad (11)$$

where $g(\mathbf{x}_k, \mathbf{r}_k, \mathbf{x}_{k-1}, \mathbf{r}_{k-1}, \mathbf{a}_k, \mathbf{b}_k)$ is equal to the last three lines in (1) (with k' replaced by k). Now marginals for individual targets used in (8) and (9) can be obtained according to $f(\mathbf{x}_k^{(j)}, r_k^{(j)} | z_{1:k}) = \int \sum_{\mathbf{r}_k^{(j)}} f(\mathbf{x}_k, r_k | z_{1:k}) d\mathbf{x}_k^{(j)}$, where $\mathbf{r}_k^{(j)}$ denotes the vector that consists of all entries in \mathbf{r}_k except $r_k^{(j)}$ and $\mathbf{x}_k^{(j)}$ denotes the vector that consists of all entries in \mathbf{x}_k except $\mathbf{x}_k^{(j)}$.

There are two interesting observations that can be made. (i) As in conventional filtering methods, by exploiting the temporal factorization structure of (1), the computational complexity can be strongly reduced. (Note that, e.g., the summation over $\sum_{\mathbf{r}_{0:k-1}}$ in (10) consists of $2^{\prod_{k'=0}^{k-1} j_{k'}}$ terms, while the k individual summations performed sequentially according to (11) only consist of $\sum_{k'=0}^{k-1} 2^{j_{k'}}$ terms.) (ii) The optimal MMSE solution is a “single scan solution” in the sense that the optimal marginal pdf $f(\mathbf{x}_k, r_k | z_{1:k})$ at time k can be directly obtained from the optimal marginal pdf $f(\mathbf{x}_{k-1}, r_{k-1} | z_{1:k-1})$ at time $k-1$, i.e., $f(\mathbf{x}_{k-1}, r_{k-1} | z_{1:k-1})$ provides all relevant information from past time steps.

BP makes it possible to also exploit the spatial factorization structure of (1) to further reduce computational complexity [5], [38]. It operates on a factor graph that represents the statistical model of the considered estimation problem [50]. In particular, marginal pdfs are calculated efficiently by performing local operations for the graph nodes and exchanging their results called “messages” along the graph edges. Since the factor graph in Fig. 1 representing this structure has cycles, BP can only provide approximate marginal pdfs $f(\mathbf{x}_k^{(j)}, r_k^{(j)} | z_{1:k})$, $j \in \{1, \dots, j_k\}$ [50]. These approximate marginal pdfs are typically referred to as “beliefs”. Furthermore, the cycles in

the factor graph lead to overconfident messages and beliefs [51], i.e., their spread “downplays” their true uncertainty.

Since BP performs marginalization similarly to JPDA, it is expected to suffer from track coalescence. However, as will be seen in Section IV, track coalescence is reduced significantly compared to JPDA. This can be explained by the particle-based implementation used by BP-based MTT that makes it possible to more accurately represent multimodal marginal pdfs. Furthermore, the overconfident nature of BP-based data association “upsells” the most likely measurement-to-target associations hypothesis and thus leads to a hybrid form of soft and hard data association and further reduces coalescence.

IV. RESULTS

We simulate three different scenarios with two targets whose states consist of two-dimensional (2D) position and velocity, i.e., $\mathbf{x}_k^{(j)} = [\mathbf{x}_{1,k}^{(j)} \ \mathbf{x}_{2,k}^{(j)} \ \dot{\mathbf{x}}_{1,k}^{(j)} \ \dot{\mathbf{x}}_{2,k}^{(j)}]^T$, $j \in \{1, 2\}$. The targets are assumed to move according to the near constant-velocity motion model, i.e., $\mathbf{x}_k^{(j)} = \mathbf{A} \mathbf{x}_{k-1}^{(j)} + \mathbf{u}_k^{(j)}$ where $\mathbf{u}_k^{(j)} \sim \mathcal{N}(\mathbf{0}, \Sigma_u)$ is a sequence of independent and identically distributed (iid) 2D Gaussian random vectors. The matrixes \mathbf{A} and Σ_u represent discretized continuous-time kinematics [52], i.e.,

$$\mathbf{A} = \begin{pmatrix} 1 & 0 & T & 0 \\ 0 & 1 & 0 & T \\ 0 & 0 & 1 & 0 \\ 0 & 0 & 0 & 1 \end{pmatrix}, \quad \Sigma_u = \begin{pmatrix} \frac{T^3}{3} & 0 & \frac{T^2}{2} & 0 \\ 0 & \frac{T^3}{3} & 0 & \frac{T^2}{2} \\ \frac{T^2}{2} & 0 & T & 0 \\ 0 & \frac{T^2}{2} & 0 & T \end{pmatrix} \sigma_u^2$$

with $\sigma_u^2 = 0.1 \text{ m}^2/\text{s}^4$ and $T = 1 \text{ s}$. The true target tracks for the three different scenarios as well as the initial target positions are shown in Fig. 2. Note that in scenarios 1 and 2, the minimum distance between the two targets is equal to σ_v (defined in what follows). The region-of-interest (ROI) is given by $[-750 \text{ m}, 750 \text{ m}] \times [-750 \text{ m}, 750 \text{ m}]$ for scenarios 1 and 3 and by $[0 \text{ m}, 1500 \text{ m}] \times [-750 \text{ m}, 750 \text{ m}]$ for scenario 2.

A single sensor performs noisy measurements of the positions of the targets. More specifically, the target-generated measurements are given by

$$\mathbf{z}_k^{(m)} = [\mathbf{x}_{1,k}^{(m)} \ \mathbf{x}_{2,k}^{(m)}]^T + \mathbf{v}_k^{(m)}$$

where $\mathbf{v}_k^{(m)} \sim \mathcal{N}(\mathbf{0}, \sigma_v^2 \mathbf{I}_2)$ with $\sigma_v = 10 \text{ m}$ is an iid sequence of 2D Gaussian random vectors. The clutter pdf $f_c(\mathbf{z}_k^{(m)})$ is uniform on the ROI. The mean number of clutter measurements is $\mu_c = 10$. A birth distribution $f_b(\mathbf{x}_{n,k})$ that is uniform on the ROI is considered. Furthermore, the mean number of newborn targets per time step and the survival probability are set to $\mu_b = 0.01$ and $p_s = 0.995$, respectively.

We use the particle-based implementation of BP for MTT presented in [38] with $J = 5000$ particles for each PT state. The threshold for target confirmation is $P_{th} = 0.5$. Potential target states are pruned if their existence probability is below threshold $P_{pr} = 10^{-5}$. We simulated 300 time steps n and 1000 Monte Carlo realizations for each of the three scenarios. We used the track-oriented variant of the MHT method. The JPDA and the MHT methods used a gate validation threshold of 13.82, which corresponds to a probability of 0.999 that target-originated measurements (when the corresponding

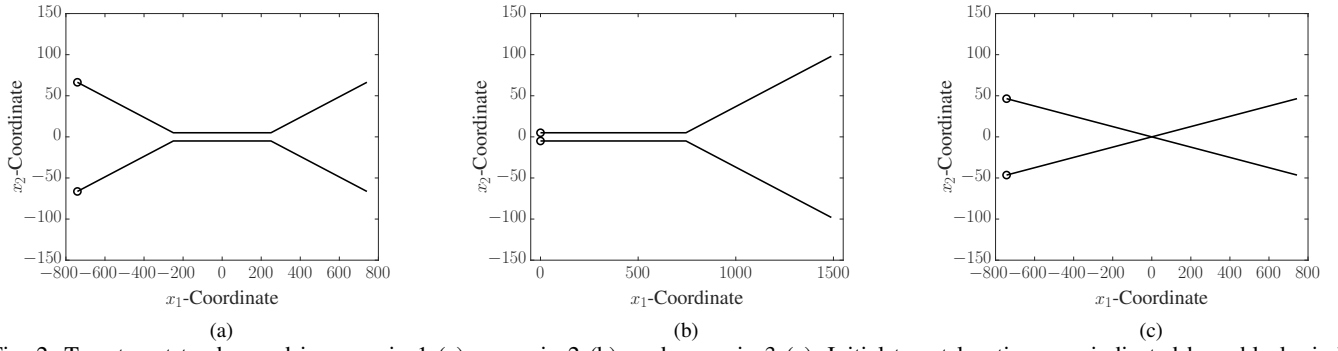


Fig. 2: True target tracks used in scenario 1 (a), scenario 2 (b), and scenario 3 (c). Initial target locations are indicated by a black circle. Note that the two coordinate axis are scaled differently.

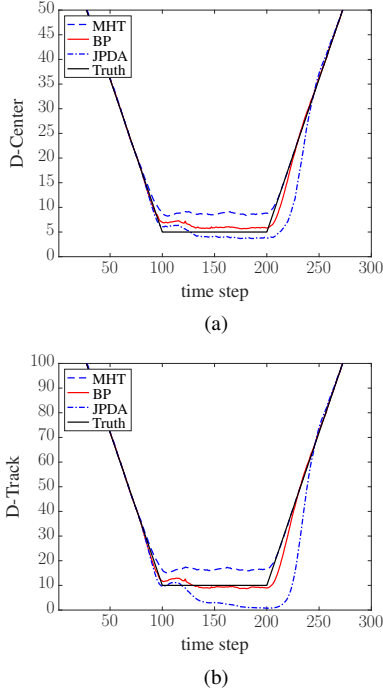


Fig. 3: Scenario 1: D-Center (a) and D-Tracks (b) for the three considered multitarget tracking methods.

target exists) are within the gate. A gate validation threshold of 9.21, which corresponds to a probability of 0.99 that target-originated measurements are within the gate, led to similar results (not shown). The track confirmation logics of JPDA and MHT are set to 10/16 and 12/24, respectively. Furthermore, the JPDA and the MHT allow at most 13 missed detections prior to track termination. These values are tuned to best represent the algorithms across all three scenarios. The hypothesis depth of the MHT filter is set to five scans.

To visualize the coalescence and repulsion effects related to the estimated tracks provided by the JPDA, MHT, and BP methods, we compute the mean distance of the estimated y-coordinates to the center between the two tracks' ("D-Center") as well as the distance between the estimated y-coordinates of the two tracks ("D-Tracks"). In particular the D-Center is the mean of $(|\hat{x}_{2,k}^{(1)}| + |\hat{x}_{2,k}^{(2)}|)/2$, averaged over all time steps and realizations. If more than two tracks are

estimated at a certain time step, then only the two estimates which are closest (in a global nearest neighbor sense) to the true tracks are considered. Similarly, if one or no tracks are estimated at certain time steps, the missing state estimates are excluded from the mean. Furthermore, D-Tracks is the mean of $|\hat{x}_{2,k}^{(1)} - \hat{x}_{2,k}^{(2)}|$, averaged over all time steps and iterations. Additional and missing tracks are handled similarly as for D-Center. D-Tracks can alert to coalescence, while (assuming tracks symmetric about the origin) D-Center examines the quality of the tracks' centroid. For example, if both are zero, the tracks may have coalesced but at least their joint track is good; but if D-Center is large then even the joint track is poor.

Fig. 3 shows D-Center and D-Tracks for scenario 1. In Fig. 3(a) it can be seen that when the two targets move in parallel and in close proximity, the tracks provided by the MHT yield an increased D-Center compared to the true tracks due to track repulsion. On the other hand, for tracks provided by the JPDA, D-Center is reduced; for time steps $200 \leq n \leq 250$, the reduced D-Center due to track coalescence is particularly pronounced after the true tracks have split again. Furthermore, it can also be observed that the tracks provided by BP only suffer from a very weak form of repulsion (when true tracks are in close proximity) and coalescence (after the true tracks have split). For the D-Tracks in 3(b), it can be seen that the track coalescence effect leads to target tracks that move towards each other until they have almost identical y-coordinates. In scenarios 2 and 3, we have observed a similar behavior of D-Center and D-Tracks (not shown).

As an additional performance metric, we use the general optimal subpattern assignment (GOSPA) [53] based on the 2-norm as inner metric as well as parameters $p = 1$ and $c = 50$. The mean GOSPA—averaged over all simulation runs—for the three tracking methods in scenario 1 is shown in Fig. 4. We show the mean total GOSPA in Fig. 4(a) as well as the individual GOSPA contributions, namely the mean total localization error, the mean missed target error, and the mean false target error in Figs. 4(b)–(d), respectively. The estimated MHT tracks yield a slightly increased total GOSPA for times $n < 100$, due to an increase number of missed tracks compared to the estimated JPDA and BP tracks. This slightly increased number of missed tracks is the result of MHT parameters that were tuned to yield satisfying performance in all three scenarios. (Note that for the JPDA method it was not possible

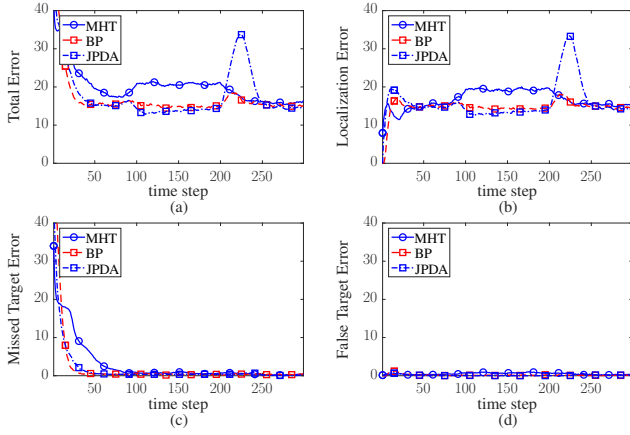


Fig. 4: Scenario 1: Mean total GOSPA (a) mean localization error (b), mean missed target error (c), and mean false target error (d) versus time for the three considered multitarget tracking methods.

to find parameters that lead to a satisfying performance in scenario 2.) For the times where the targets are in close proximity, i.e., $100 \leq n \leq 200$, coalescence of estimated JPDA tracks results in a lower localization error compared to the other time steps and compared to the other methods. However, right after the true target tracks split, i.e., at times $200 < n < 240$, the JPDA yields a significant localization error peak. Due to track repulsion, the localization error of estimated MHT tracks is increased when targets are in close proximity. Notably, the localization error related to BP is significantly reduced compared to the other two methods.

Fig. 5 shows the mean GOSPA error of the JPDA, MHT, and BP methods in scenario 2. For time steps where targets are in close proximity, i.e., $0 \leq n \leq 150$, due to track repulsion, the localization and total GOSPA errors of the MHT are increased compared to those of the BP method. In addition, it can be seen that for times $n < 150$, the missed target and total GOSPA errors of the JPDA result are significantly increased compared to the other two methods. This is because the confirmation logic of the JPDA is unable to initialize two tracks as long the true target states remain in close proximity [1]. The fact that the JPDA only creates a single track for these time steps, results in a reduced localization error compared to MHT and BP. As expected this localization error is 5m on average, which is equal to half the distance between the two tracks. In scenario 2, BP yields a slightly increased false tracks error compared to JPDA and MHT. This increased error is mostly due the generation of short tracks that only consists of few time steps and could be removed in post-processing. (Note that the tracking confirmation logics used for JPDA and MHT automatically suppress such short tracks.)

Finally, Fig. 6 shows the mean GOSPA error of the JPDA, MHT, and BP methods in scenario 3. Here we can again see that for time steps where targets are in close proximity, i.e., $125 \leq n \leq 175$, due to track repulsion, the localization and total GOSPA error of MHT is increased compared to the other methods. On the other hand, track coalescence of the JPDA decreases the localization and total GOSPA error when targets

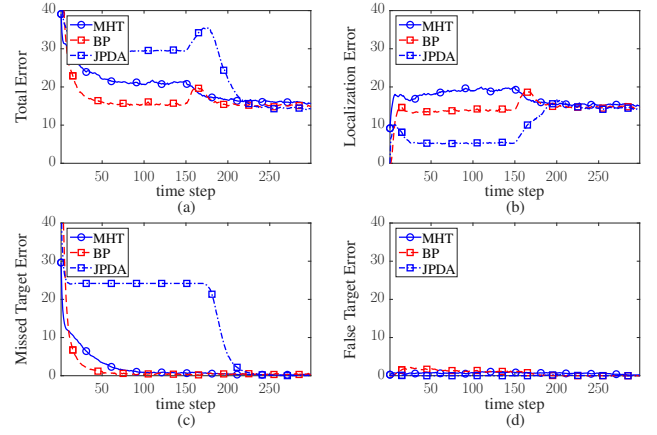


Fig. 5: Scenario 2: Mean total GOSPA (a) mean localization error (b), mean missed target error (c), and mean false target error (d) versus time for the three considered multitarget tracking methods.

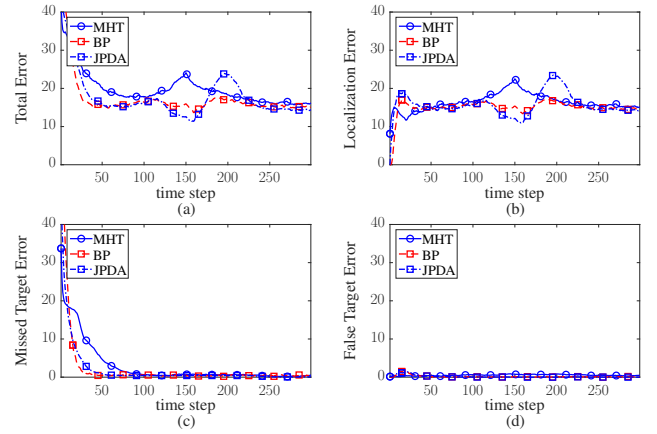


Fig. 6: Scenario 3: Mean total GOSPA (a) mean localization error (b), mean missed target error (c), and mean false target error (d) versus time for the three considered multitarget tracking methods.

are in close proximity ($125 \leq n \leq 175$) and increases them right after the two targets have split ($175 \leq n \leq 225$). An important aspect in a scenario with crossing tracks are track swaps [45]. A quantification of track swaps based on track-level metrics [44] will be reported in future work.

V. CONCLUSION

In this paper, we reviewed the estimation strategies of multiple hypothesis tracking (MHT), joint probabilistic data association (JPDA), and the recently introduced belief propagation (BP) approach for MTT. Since BP performs marginalization similarly to JPDA, it is expected to suffer from track coalescence. Our results however indicated that BP-based MTT can mostly avoid coalescence and repulsion, problems that respectively afflict JPDA and MHT. This can be explained by the particle-based implementation used by BP-based MTT that makes it possible to accurately represent multimodal marginal pdfs. Furthermore, the overconfident nature of BP-based data association “upsells” the most likely measurement-to-target associations hypothesis and thus leads to a hybrid form of soft and hard data association that reduces track coalescence.

REFERENCES

- [1] Y. Bar-Shalom, P. K. Willett, and X. Tian, *Tracking and Data Fusion: A Handbook of Algorithms*. Storrs, CT: Yaakov Bar-Shalom, 2011.
- [2] S. Challa, M. R. Morelande, D. Mušicki, and R. J. Evans, *Fundamentals of Object Tracking*. Cambridge, UK: Cambridge University Press, 2011.
- [3] R. Mahler, *Statistical Multisource-Multitarget Information Fusion*. Norwood, MA: Artech House, 2007.
- [4] W. Koch, *Tracking and Sensor Data Fusion: Methodological Framework and Selected Applications*. Berlin, Germany: Springer, 2014.
- [5] F. Meyer, T. Kropfreiter, J. L. Williams, R. Lau, F. Hlawatsch, P. Braca, and M. Z. Win, "Message passing algorithms for scalable multitarget tracking," *Proc. IEEE*, vol. 106, no. 2, pp. 221–259, 2018.
- [6] D. B. Reid, "An algorithm for tracking multiple targets," *IEEE Trans. Autom. Control*, vol. 24, no. 6, pp. 843–854, Dec. 1979.
- [7] Y. Bar-Shalom, "Extension of the probabilistic data association filter in multi-target tracking," in *Proc. SNETA-74*, San Diego, CA, Sep. 1974.
- [8] Y. Bar-Shalom, F. Daum, and J. Huang, "The probabilistic data association filter," *IEEE Control Syst. Mag.*, vol. 29, pp. 82–100, Dec. 2009.
- [9] T. Fortmann, Y. Bar-Shalom, and M. Scheffe, "Sonar tracking of multiple targets using joint probabilistic data association," *IEEE J. Ocean. Eng.*, vol. 8, no. 3, pp. 173–184, Jul. 1983.
- [10] G. Ferri, A. Munafo, A. Tesei, P. Braca, F. Meyer, K. Pelekanakis, R. Petrocchia, J. Alves, C. Strode, and K. LePage, "Cooperative robotic networks for underwater surveillance: an overview," *IET Radar Sonar Navig.*, vol. 11, no. 12, pp. 1740–1761, 2017.
- [11] D. Y. Kim, B. Ristic, R. Guan, and L. Rosenberg, "A Bernoulli track-before-detect filter for interacting targets in maritime radar," *IEEE Trans. Aerosp. Electron. Syst.*, pp. 1–10, Jan. 2021.
- [12] J. Levinson and al., "Towards fully autonomous driving: Systems and algorithms," in *Proc. IEEE IV 2011*, Baden-Baden, Germany, Jun. 2011, pp. 163–168.
- [13] F. Meyer and J. L. Williams, "Scalable detection and tracking of geometric extended objects," 2021, arXiv:2103.11279.
- [14] D. Musicki and R. Evans, "Joint integrated probabilistic data association: JIPDA," *IEEE Trans. Aerosp. Electron. Syst.*, vol. 40, no. 3, pp. 1093–1099, Jul. 2004.
- [15] J. Vermaak, S. Maskell, and M. Briers, "A unifying framework for multi-target tracking and existence," in *Proc. FUSION-05*, Philadelphia, PA, Jul. 2005, pp. 250–258.
- [16] Musicki, D. and La Scala, B., "Multi-target tracking in clutter without measurement assignment," *IEEE Trans. Aerosp. Electron. Syst.*, vol. 44, no. 3, pp. 877–896, Jul. 2008.
- [17] P. Horridge and S. Maskell, "Real-time tracking of hundreds of targets with efficient exact JPDAF implementation," in *Proc. FUSION-06*, Florence, Italy, Jul. 2006.
- [18] K. Pattipati, R. L. Popp, and T. Kirubarajan, "Survey of assignment techniques for multitarget tracking," in *Multitarget-Multisensor Tracking: Applications and Advances*, Y. Bar-Shalom and W. D. Blair, Eds. Norwood, MA: Artech-House, 2000, vol. 3, ch. 2, pp. 77–159.
- [19] I. J. Cox and S. L. Hingorani, "An efficient implementation of Reid's multiple hypothesis tracking algorithm and its evaluation for the purpose of visual tracking," *IEEE Trans. Pattern Anal. Mach. Intell.*, vol. 18, no. 2, pp. 138–150, Feb. 1996.
- [20] R. Danchick and G. E. Newnam, "Reformulating Reid's MHT method with generalised Murty K-best ranked linear assignment algorithm," *IEE Radar Sonar Navig.*, vol. 153, no. 1, pp. 13–22, Feb. 2006.
- [21] T. Kurien, "Issues in the design of practical multitarget tracking algorithms," in *Multitarget-Multisensor Tracking: Advanced Applications*, Y. Bar-Shalom, Ed. Norwood, MA: Artech-House, 1990, pp. 43–83.
- [22] S. S. Blackman, "Multiple hypothesis tracking for multiple target tracking," *IEEE Trans. Aerosp. Electron. Syst.*, vol. 19, pp. 5–18, Jan. 2004.
- [23] C. Morefield, "Application of 0-1 integer programming to multitarget tracking problems," *IEEE Trans. Autom. Control*, vol. 22, no. 3, pp. 302–312, Jun. 1977.
- [24] S. Deb, M. Yeddnapudi, K. Pattipati, and Y. Bar-Shalom, "A generalized S-D assignment algorithm for multisensor-multitarget state estimation," *IEEE Trans. Aerosp. Electron. Syst.*, vol. 33, no. 2, pp. 523–538, Apr. 1997.
- [25] R. P. S. Mahler, "Multitarget Bayes filtering via first-order multitarget moments," *IEEE Trans. Aerosp. Electron. Syst.*, vol. 39, no. 4, pp. 1152–1178, Oct. 2003.
- [26] B.-N. Vo, S. Singh, and A. Doucet, "Sequential Monte Carlo methods for multitarget filtering with random finite sets," *IEEE Trans. Aerosp. Electron. Syst.*, vol. 41, no. 4, pp. 1224–1245, Oct. 2005.
- [27] B.-T. Vo, B.-N. Vo, and A. Cantoni, "Analytic implementations of the cardinalized probability hypothesis density filter," *IEEE Trans. Signal Process.*, vol. 55, no. 7, pp. 3553–3567, Jul. 2007.
- [28] J. L. Williams, "Marginal multi-Bernoulli filters: RFS derivation of MHT, JIPDA and association-based MeMBer," *IEEE Trans. Aerosp. Electron. Syst.*, vol. 51, no. 3, pp. 1664–1687, Jul. 2015.
- [29] S. Nannuru, S. Blouin, M. Coates, and M. Rabbat, "Multisensor CPHD filter," *IEEE Trans. Aerosp. Electron. Syst.*, vol. 52, no. 4, pp. 1834–1854, Aug. 2016.
- [30] R. J. Fitzgerald, "Track biases and coalescence with probabilistic data association," *IEEE Trans. Signal Process.*, vol. 21, no. 6, pp. 822–825, Nov. 1985.
- [31] S. Coraluppi, C. Carthel, P. Willett, M. Dingboe, O. O'Neill, and T. Luginbuhl, "The track repulsion effect in automatic tracking," in *Proc. FUSION-09*, Seattle, WA, USA, Jul. 2009, pp. 2225–2230.
- [32] H. Blom and E. Bloem, "Probabilistic data association avoiding track coalescence," *IEEE Trans. Autom. Control*, vol. 45, no. 2, pp. 247–259, Feb. 2000.
- [33] H. A. P. Blom, E. A. Bloem, and D. Musicki, "JIPDA: Automatic target tracking avoiding track coalescence," *IEEE Trans. Aerosp. Electron. Syst.*, vol. 51, no. 2, pp. 962–974, Apr. 2015.
- [34] S. Coraluppi and C. Carthel, "An equivalence-class approach to multiple-hypothesis tracking," in *Proc. AeroConf-12*, Big Sky, MT, USA, Mar. 2012, pp. 1–8.
- [35] L. Svensson, D. Svensson, M. Guerriero, and P. Willett, "Set JPDA filter for multitarget tracking," *IEEE Trans. Signal Process.*, vol. 59, no. 10, pp. 4677–4691, Oct. 2011.
- [36] S. Reuter, B.-T. Vo, B.-N. Vo, and K. Dietmayer, "The labeled multi-Bernoulli filter," *IEEE Trans. Signal Process.*, vol. 62, no. 12, pp. 3246–3260, Jun. 2014.
- [37] J. L. Williams and R. Lau, "Approximate evaluation of marginal association probabilities with belief propagation," *IEEE Trans. Aerosp. Electron. Syst.*, vol. 50, no. 4, pp. 2942–2959, Oct. 2014.
- [38] F. Meyer, P. Braca, P. Willett, and F. Hlawatsch, "A scalable algorithm for tracking an unknown number of targets using multiple sensors," *IEEE Trans. Signal Process.*, vol. 65, no. 13, pp. 3478–3493, Mar. 2017.
- [39] F. Meyer, O. Hlinka, H. Wymeersch, E. Riegler, and F. Hlawatsch, "Distributed localization and tracking of mobile networks including noncooperative objects," *IEEE Trans. Signal Inf. Process. Netw.*, vol. 2, no. 1, pp. 57–71, Mar. 2016.
- [40] K. R. Pattipati, S. Deb, Y. Bar-Shalom, and R. B. J. Washburn, "A new relaxation algorithm and passive sensor data association," *IEEE Trans. Autom. Control*, vol. 37, no. 2, pp. 198–213, Feb. 1992.
- [41] A. P. Poore and N. Rijavec, "A Lagrangian relaxation algorithm for multidimensional assignment problems arising from multitarget tracking," *SIAM J. Optimiz.*, vol. 3, no. 3, pp. 544–563, 1993.
- [42] A. B. Poore and S. Gadaleta, "Some assignment problems arising from multiple target tracking," *Math. Comput. Model.*, vol. 43, no. 9–10, pp. 1074–1091, 2006.
- [43] S. Mori, C.-Y. Chong, and K. C. Chang, "Evaluation of data association hypotheses: Non-Poisson i.i.d. cases," in *Proc. FUSION-04*, Stockholm, Sweden, Jun. 2004.
- [44] S. Coraluppi, D. Grimmer, and P. de Theije, "Benchmark evaluation of multitactic trackers," in *Proc. FUSION-06*, Florence, Italy, Jul. 2006.
- [45] P. Willett, T. Luginbuhl, and E. Giannopoulos, "MHT tracking for crossing sonar targets," in *Proc. SPIE*, San Diego, CA, USA, Sep. 2007, pp. 469–480.
- [46] R. Fitzgerald, "Development of practical PDA logic for multitarget tracking by microprocessor," in *Multitarget-Multisensor Tracking: Advanced Applications*, Y. Bar-Shalom, Ed. Norwood, MA: Artech-House, 1990.
- [47] J. L. Williams, "An efficient, variational approximation of the best fitting multi-Bernoulli filter," *IEEE Trans. Signal Process.*, vol. 63, no. 1, pp. 258–273, Jan. 2015.
- [48] R. A. Lau and J. L. Williams, "A structured mean field approach for existence-based multiple target tracking," in *Proc. FUSION-16*, Heidelberg, Germany, Jul. 2016, pp. 1111–1118.
- [49] G. Soldi, F. Meyer, P. Braca, and F. Hlawatsch, "Self-tuning algorithms for multisensor-multitarget tracking using belief propagation," *IEEE Trans. Signal Process.*, vol. 67, no. 15, pp. 3922–3937, Aug. 2019.
- [50] F. R. Kschischang, B. J. Frey, and H.-A. Loeliger, "Factor graphs and the sum-product algorithm," *IEEE Trans. Inf. Theory*, vol. 47, no. 2, pp. 498–519, Feb. 2001.
- [51] Y. Weiss and W. T. Freeman, "Correctness of belief propagation in Gaussian graphical models of arbitrary topology," *Neural Comput.*, vol. 13, no. 10, pp. 2173–2200, 2001.
- [52] Y. Bar-Shalom, T. Kirubarajan, and X.-R. Li, *Estimation with Applications to Tracking and Navigation*. New York City, NY: Wiley, 2002.
- [53] A. S. Rahmathullah, Á. F. García-Fernández, and L. Svensson, "Generalized optimal sub-pattern assignment metric," in *Proc. FUSION-17*, Xi'an, China, Jul. 2017.